# Chapter III: Glomerular Structure of the AT1a Receptor Deficient Mice

## Summary

The angiotensin II type1a (AT1a) receptor is the major receptor effecting the multiple actions of angiotensin II on the cardiovascular system. It is expressed abundantly in the glomerular mesangial cells of the kidney. We investigated glomerular changes in null mutant mice minus the AT1a receptor gene to gain an understanding of the in vivo action of angiotensin II via AT1a on the mesangium. Morphological observations and morphometric analysis revealed that the glomerular volume was greatly increased owing to the expansion of the mesangial area, which contained fluid filled spaces with a small amount of fibrillar components. The mesangial cells lost contact with each other and with the perimesangial area of the glomerular basement membrane (GBM), so that the glomerular capillary neck was greatly widened. These findings suggest a defect of the anchoring function of mesangial cells resulting from some abnormality in mesangial matrix formation. We conclude that angiotensin II has an important role in the structural and functional maintenance of the mesangium via the AT1a receptor, especially by reinforcing the connection between mesangial cells and GBM via the mesangial matrix.

# Introduction

Angiotensin II has various important roles in cardiovascular regulation, mainly via type 1 (AT1) receptor. AT1 receptors have been shown to be expressed abundantly in the mesangial cells [19,33,39] and to have two isoforms, AT1a and AT1b. AT1a receptors have been reported to predominate in producing effects of angiotensin II [19], which regulates the glomerular filtration rate [ 22, 25, 37, 47], and modulates the ultrafiltration coefficient by contraction of mesangial cells [22, 37]. The phenotype of mesangial cells, however, differs from that of smooth muscle cells, and they appear to be unable to contract as smooth muscles do [34]. Angiotensin II has been shown to stimulate the synthesis of mesangial extracellular matrices [ 41, 49], mesangial cell proliferation [40, 41, 48, 49] and mesangial cell hypertrophy [21,48] in experiments using in vitro-cultured mesangial cells. However, the in vivo action of angiotensin II on glomerular mesangial cells via AT1a has not been clarified yet.

In this study, we investigated the glomerular changes in null mutant mice minus the AT1a receptor gene to gain an underatanding of the in vivo action of angiotensin II on the glomerular mesangium via AT1a receptor. We visualized extracellular matrices and the intracellular fibrillar structure at the electron microscopic level [42,43], and morphological and morphometric analysis enabled us to gain a thorough understanding of angiotensin II actions in mesangial function.

## Materials and Methods

We used homozygous AT1a gene-deficient mice (AT1a null mutant mice) generated from C57BL/6 mice [19]. In the mutant mice, the AT1a receptor gene was disrupted by replacement with the ß-galactosidase (lacZ) gene. The null mutant mice displayed hypotension and hyper-reninaemia [19]. C57BL/6 mice of the wild type were used as control mice.

Four null mutant mice, two each aged 8 and 27 weeks, and four wild-type mice of the same ages were used for morphological examination. The mice were anaesthetized by intraperitoneal injection of a mixture of ketamine (Ketarar 50, Sankyo, Tokyo, Japan) and xyladine (Ceraktar, Bayer Japan, Tokyo, Japan). After opening the abdominal cavity, the abdominal aorta was cannulated with a retrograde catheter, and perfused by a fixative for 5 min with a perfusion apparatus (Kosaka Laboratory, Tokyo, Japan) operated at a pressure of about 200-220 mmHg for the null mutant mice and about 200-250 mmHg for the control mice. The fixative contained 2% glutaraldehyde in 0.1 M cacodylate buffer at pH 7.4. Small pieces of cortical tissue were processed by a cold-dehydration technique [42]. After brief treatment with 0.1% osmium tetroxide, the blocks were stained en bloc with 1% tannic acid and uranyl acetate successively. The blocks were then dehydrated in a graded series of acetone at gradually decreasing temperatures down to -30°C and embedded in Epon 812. These procedures enabled detailed morphological observation of the extracellular matrix and intracellular fibrillar structures [42]. Semithin sections (1mm) were stained with toluidine blue and prepared for light microscopy. Ultrathin sections were stained with uranyl acetate and lead citrate and were examined with a JEM-1200EX electron microscope (JEOL, Tokyo, Japan).

To guantitate the glomerular changes, the glomerular tuft volume as and the volumes and surface areas of their components, including the glomerular basement membrane (GBM)

surface area, were determined by means of a combination of light microscopic and electron microscopic morphometry, as described elsewhere [27, 43]. Briefly, the glomerular tuft volume in each kidney was estimated on the basis of light microscopic measurement of 50 random sectional profiles of glomeruli in semithin sections. The relative volumes and surface areas of each component of glomeruli per glomerular tuft volume were determined on the basis of electron microscopic measurement of 5 equatorial sectional profiles of glomeruli in ultrathin sections. The absolute volumes or surface areas of each component of glomeruli were determined as products of the glomerular tuft volume and their relative volumes or surface areas, respectively.

To estimate the glomerular tuft volume [V(T)], we determined the mean tuft area [A(T)], which was defined as the average of the domain areas of minimal convex polygon circumscribing all tuft components in sections including capillaries, mesangium, podocytes and narrow urinary spaces. The measurements were made taken with the aid of a semiautomatic image analysis system (IBAS, Carl Zeiss, Oberkohen, Germany) connected to a photomicroscope. Outlines of the profiles on a video monitor were traced on a digitizing tablet at x 1000 magnification. The glomerular tuft volume was calculated from [A(T)] using the formula;

$$V(T)=b/K\ A(T)^{(3/2)},$$

where b is the shape coefficient for spheres and K is the distribution coefficient [30, 46].

The relative volumes of individual components ( volume density; Vv) were represented by their domain area divided by the tuft domain area (AA). The relative surface areas of individual components (surface density; Sv) were calculated from their border lengths divided by the tuft domain area (LA) using the formula;

$Sv = 4\ LA / p.$

The volume of each tuft component [V(C)] , that is, inner GBM volume, capillary volume and mesangial volume, was calculated using the formula;

$V(C) = V(T) \times Vv.$

The glomerular tuft volume is defined as the volume of the minimal convex polyhedron containing the total tuft structure, and is therefore much larger than the inner GBM volume. The inner GBM volume consists of the capillary volume and the mesangial volume.

The surface area of each tuft component [S(C)], that is, total GBM, pericapillary GBM and perimesangial GBM surface area, was calculated from the formula;

$S(C) = V(T) \times Sv.$

The GBM surface area is composed of that of two subdomains, namely the pericapillary and perimesangial GBM surface areas. The two subdomains are demarcated from each other by the mesangial angle.

Individual glomerular components were identified on glomerular profiles printed at a final magnification of x 1500 of transmission electron micrographs, and their domain areas and border lengths were measured by means of a digitizer and a computer software for image analysis (Cosmozone software, Nikon, Tokyo, Japan).

Morphometric data were analyzed by computer software for statistical analysis (Stat-View II , Abacus Concepts, Berkeley, Calif.). Values are presented as mean ± standard deviation. One-way analysis of a variance (ANOVA) was performed among four groups. When the difference was significant, Sheffe's multiple comparison test was performed to identify which groups were statistically different from which others

# Results

Glomerular profiles in the wild-type mice at the ages of 8 (Fig. 5a) and 27 weeks (Fig. 5c) were composed of many glomerular capillary loops and small amounts of mesangium connecting them. In the null mutant mice at the ages of 8 (Fig.5b) and 27 weeks (Fig. 5d) they were markedly enlarged compared with those in the wild-type mice of the same age (Figs. 5a, 5c). The most prominent morphological change of enlarged glomeruli in the null mutant mice was the increase in the absolute mesangial area and widening of the glomerular hilum (Fig. 5d). The enlarged space between the afferent and efferent arterioles was occupied by increased intercellular space and a number of cells of extraglomerular mesangium. Foot processes of glomerular epithelial cells in the null mutant mice at the ages of 8 and 27 weeks were well preserved and appeared equal in size to those in corresponding wild-type mice. Glomerular basement membrane in the null mutant mice at the ages of 8 and 27 weeks was of the same thickness as in the corresponding wild-type mice.

The structure of the glomerular tufts in the wild-type mice showed a few mesangial cells, with a small amount of mesangial matrix around them and narrow capillary necks(Fig. 6a). The mesangial cell processes were anchored to the GBM and thus kept the capillary necks restricted. The structure of the tufts in the null mutant mice varied among the glomeruli and within a single glomerulus and showed three types of morphological changes, although it is impossible to define their boundaries : mesangial enlargement, moderate increase of mesangial matrix together with widening of the capillary neck (Fig. 6b); mesangial dissolution with extreme expansion of the mesangial matrix area characterized by fluid-filled spaces with a small amount of fibrillar components (Fig. 6c); and mesangial interposition, a slightly expanded

mesangium which contains mesangial cells surrounding individual capillaries (Fig. 6d). In these glomerular areas with structural changes of mesangial enlargement, the mesangial matrix area was moderately enlarged and contained loosely packed extracellular matrices, including flocculent materials and scattered thick fibrils.

At the age of 8 weeks, in the null mutant mice mesangial enlargement was observed in almost every glomerulus and occupied about three quarters of the glomerular area. An area of mesangial dissolution was also observed in almost every glomerulus and occupied about one quarter of the glomerular area in the null mutant mice. There was no mesangial interposition in the null mutant mice at this age. By the age of 27 weeks, mesangial enlargement was observed in one quarter of the glomerular area, and the glomerular area of mesangial dissolution occupied about three quarters of the glomerular area in the null mutant mice. Mesangial interposition was found in only a few glomeruli in the null mutant mice and the proportion of this type of mesangial area was quite variable among glomeruli.

In the null mutant mice, mesangial dissolution was the most characteristic alteration. In these, the mesangial matrix area was greatly enlarged and contained an abundance of fluid-filled space and a small amount of extracellular matrix (Fig.7a). The individual mesangial cells were separated from the GBM or endothelial cells by the fluid-filled spaces(Fig. 7b). In the mesangial dissolution area, the capillary diameter was variable. The capillaries in the peripheral glomerular tuft were segmentally enlarged (Fig. 7a, capillary lumen shown as L). Capillary endothelial cells were occasionally separated from the GBM by the fluid-filled spaces. The endothelial cells facing the fluid-filled spaces had a wavy outline and were separated from the fluid-filled spaces by an incomplete sheet of basal lamina consisting of electron-dense material (Fig.3b arrowheads). Mesangial cell processes in the null mutant mice loss their anchoring to

the GBM over a wide area (Fig. 7b), while the mesangial cell processes in the wild-type mice were characteristically anchored to the GBM (Fig. 6a). Shreds of matrix material including assemblies of disconnected microfibrils were found within the greatly expanded intercellular spaces (Fig. 7b). Dissolutions of mesangial cell-GBM connections at mesangial angles allowed expansion of the mesangium into the space between the GBM and the capillary endothelium. The capillaries lost their narrow necks and were progressively encompassed by the mesangium. In advanced cases, these capillary profiles were encountered; they lost almost all their relationships to the GBM and, instead, were completely incorporated into the expanded mesangium (Fig. 6c).

Intracellular fibrillar structures, especially the microfilaments of mesangial cells, were rarely observed in the processes that had lost contact with the GBM in the null mutant mice (Fig. 7a).

Morphometric analysis of glomeruli revealed that glomerular tuft volume was considerably larger in the null mutant mice than in the wild-type mice (Table 1). The glomerular tuft volumes in the null mutant mice were about 3.4 times as large at 8 weeks and 2.5 times as large at 27 weeks as in the corresponding wild-type mice. The increment of glomerular tuft volume was attributed primarily to the increased mesangial volume; the proportions of mesangial volume in the glomerular tuft volume were 67% at 8 weeks and 77% at 27 weeks in the null mutant mice, while they were 34 and 43% in the corresponding wild-type mice, respectively. The mesangial volumes in the null mutant mice were about 7.6 times as larger at 8 weeks and about 5.6 times as large at 27 weeks as in the corresponding wild-type mice.

The total GBM surface area was increased moderately in the null mutant mice compared with that in the wild-type mice, both at 8 and 27 weeks. The two compartments of the total

GBM surface area, the pericapillary GBM surface area and perimesangial GBM surface area, were also larger in the null mutant mice than in the wild-type mice. The pericapillary GBM surface area in the null mutant mice was smaller by 73% at 27 weeks than at 8 weeks ($p<0.01$), while the pericapillary GBM surface areas in the wild-type mice were similar at both ages. In contrast, the perimesangial GBM areas showed no significant difference between 8 and 27 weeks in either the null mutant or wild-type mice.

# Discussion

In this study, we used a cold dehydration technique in processing the kidney tissue for transmission electron microscopy; with this the extra- and intracellular filamentous structures are better preserved much than with conventional methods [42]. This technical improvement allowed us to show that in null mutant mice, the glomerular volume was dramatically increased owing to extreme expansion of the mesangial area. In the null mutant mice, the expanded mesangial matrix area contained a grat deal of fluid-filled space and a small amount of extracellular matrix. The individual mesangial cells were separated from the GBM or endothelial cells by these fluid-filled spaces.

AT1 receptor is expressed abundantly in the mesangial cells of the kidney [ 19,33,39]. The administration of angiotensin II has been reported to stimulate the synthesis of components of the extracellular matrix in mesangial cells and smooth muscle cells in vitro [ 41, 49]. Ray et al. suggested that angiotensin II binding to AT1 receptors directly stimulates fibronectin production and cellular proliferation in cultured human fetal mesangial cells, and that the AT1 receptor subtype may well be involved in the regulation of fibronectin synthesis during development and in diseases [41]. Recent studies have suggested that some of the pathophysiologic actions of angiotensin II result from its stimulation of TGF-ß expression [28, 35, 44], which has multiple effects on glomerular cell functions including modulation of the synthesis of extracellular matrix proteins [23, 26, 36]. However, these results were obtained from in vitro studies, and the in vivo action of angiotensin II on the mesangial cells via AT1a receptor has not been clarified. Indeed it is impossible to clarify in vivo actions directly. Using angiotensin-converting enzyme inhibitors or angiotensin II receptor antagonists, it is possible to

suppress angiotensin II action in the tissue, but not to block it totally. Therefore, in this study, we used homozygous AT1a null mutant mice as a tool to gain an understanding of the in vivo action of angiotensin II on mesangial cells.

In null mutant mice, the mesangial area was greatly expanded and the mesangial matrix decreased in density. This decrease is thought to be caused by a combination of reductions in synthesis of the mesangial matrix components and in the density of the mesangial matrix by expansion of mesangial intercellular space. The expansion of these spaces per se is thought to result from inadequate anchoring of mesangial cells, probably caused by a defect in the production of extracellular matrix. The expansion of the mesangial intercellular spaces found in this study could not be resulted artificially from the perfusion pressure during the fixation, according to our preliminary study. Morphological changes in null mutant mice perfused by a physiological low pressure (110 mmHg) were fundamentally the same as in the present study (unpublished data).

This study clearly shows that the mesangial matrix components in null mutant mice cannot connect the mesangial cells firmly to the GBM or endothelial cells. We suggest that the mesangial cells in null mutant mice fail to form normal mesangial matrices and to maintain a normal mesangial structure. We suggest that the role of angiotensin II in the mesangial cells is to synthesize mesangial components, via AT1a and through AT1a to maintain the normal structure of the mesangium. Recent studies in cultured mesangial cells support our hypothesis [41, 49].

Mesangial alterations in the null mutant mice at 8 and 27 weeks were of three types: mesangial enlargement, mesangial dissolution and mesangial interposition. At 8 weeks, mesangial enlargement occupied the larger part of each glomerular area, and mesangial

dissolution occupied a minor portion. At 27 weeks, the ratio of the two types of glomerular alterations in each glomerulus was inverted. Mesangial interposition was seen in a few glomeruli only at 27 weeks. We suggest that mesangial enlargement is the earliest change and leads to mesangial dissolution, after which mesangial interposition occurs. We hypothesize that the mesangial area in null mutant mice is extended by the distending forces of blood pressure, as mesangial matrix formation is impaired, and the mesangial cells do not interconnect with each other or anchor to the GBM. We assume that mesangial interposition plays a part in preserving the mesangial structure, as a mesangial area with insufficient matrix is unable to maintain the normal mesangial structure.

It is interesting to note that the pericapillary GBM surface area in the null mutant mice was amaller at 27 weeks than at 8 weeks. In the null mutant mice, the area of mesangial dissolution was widespread at 27 weeks. The disconnection of mesangial cells and the GBM at mesangial angles allowed mesangial expansion into the space between the GBM and capillary endothelium. We assume that the capillary GBM is changed to mesangial GBM in time and thus the pericapillary GBM surface area decreased in the null mutant mice by 27 weeks of age.

In the null mutant mice, foot processes were regular in width and appeared to be identical to those of the wild-type mice. The GBM was the same thickness in the null mutant and wild-type mice. The function of the glomerular epithelial cells was thus probably normal.

Although the AT1a receptor predominate in mouse kidney, renin and angiotensin production is up-regulated in the null mutant mice and plasma angiotensin II concentration is increased. So it is conceivable that the other angiotensin II receptors, including AT1b and AT2, compensate for the lost functions of AT1a. However, the amount of AT1b receptors in AT1a null-mutant mouse kidney remains at an undetectably low level for binding autoradiography or

in situ hybridization [19,32]. It is reported that AT1b null mutant mice and AT2 null-mutant mice show no morphological abnormalities [24,29,31], but angiotensinogen null mutant mice have mesangial expansion [38]. This suggests that the glomerular changes observed in AT1a null mutant mice reflect a lack of the AT1a receptor functions. We conclude that angiotensin II plays an important part in the structural and functional maintenance of the mesangium through the AT1a receptor, including the synthesis of mesangial matrix and connection of the mesangial cells to the GBM. A future study will addressed the biochemical analysis of mesangial matrix components and AT1a gene transfer to the null mutant mesangial cells in vivo, which may provide us with further evidence for our hypothesis.

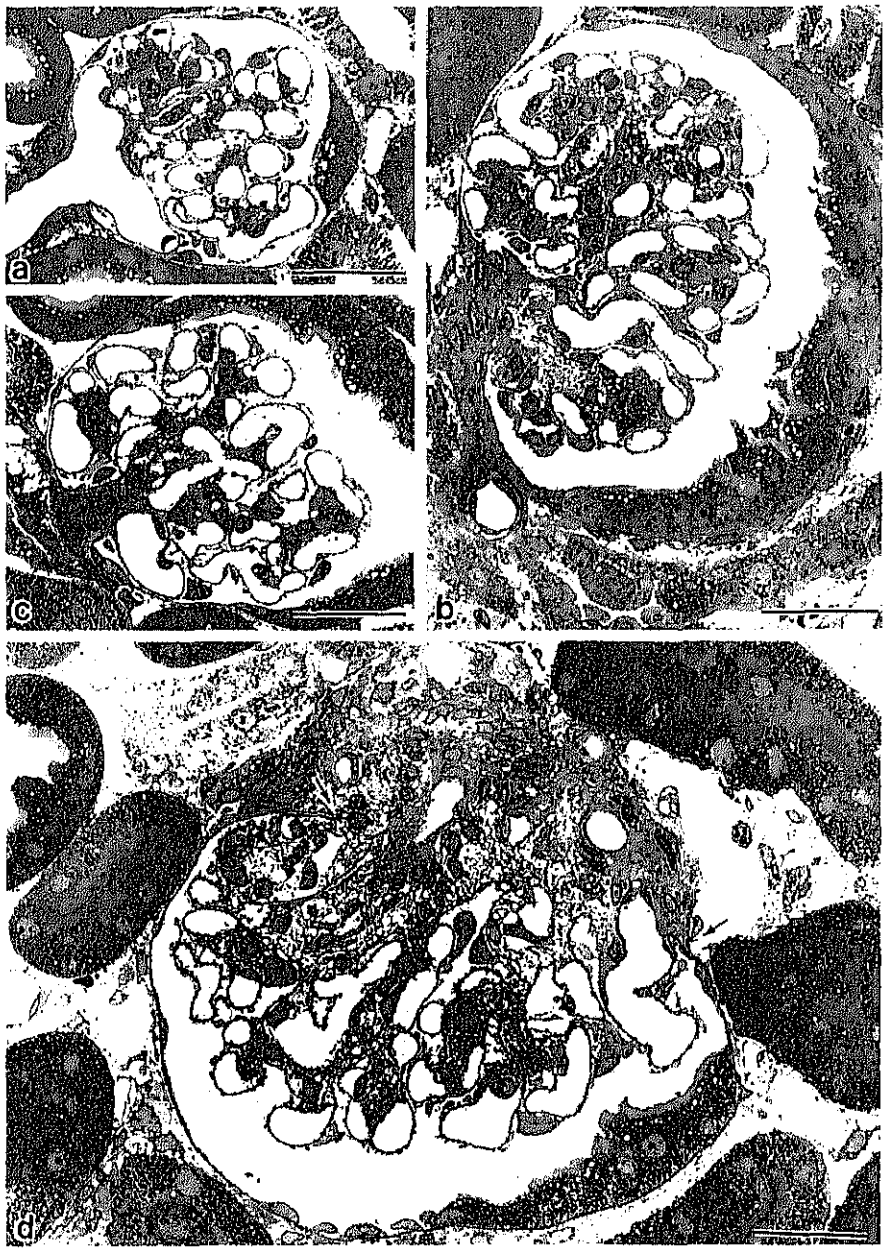


Fig. 5. Transmission electron micrograph showing glomeruli of the wild-type mice at **a** 8 and c 27 weeks after birth and the null mutant mice at **b** 8 and d 27 weeks. **a** The glomerulus was 75 μm in diameter in the wild-type mouse 8 weeks after birth and was made up of many glomerular capillary loops and a small amount of mesangium connecting them. **b** The glomerulus was larger, 100 μm in diameter, in the null mutant mouse at 8 weeks than in the corresponding wild-type mouse, an enlargement resulting from an increase in the mesangial area. **c** The glomerulus of the wild-type mouse at 27 weeks appeared the same as that of the wild-type mouse at 8 weeks, although it was slightly enlarged, 85 μm in diameter. **d** The glomerulus of the null mutant mouse at 27 weeks was markedly enlarged, 135 μm in diameter; the glomerular mesangium and extraglomerular mesangium were expanded. The glomerular hilum (between the *arrows*) was widely spread. *Bars* in the *panels* 30 μm

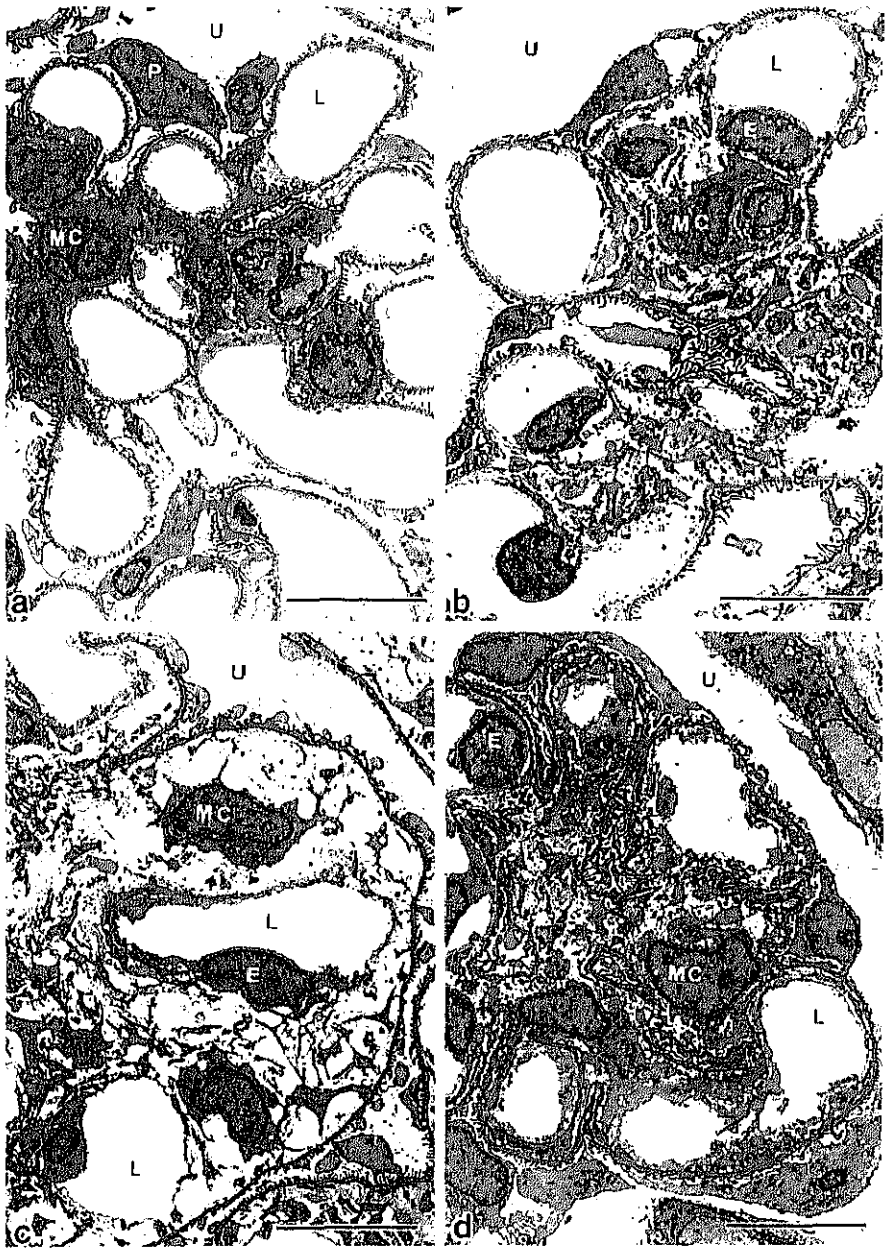


Fig. 6. a–d Three types of mesangial alterations in the null mutant mice. a The mesangium from the wild-type mouse was composed of a few mesangial cells and a small amount of mesangial matrix surrounding the mesangial cells. b–d In contrast, the mesangium of the null mutant mice showed three types of alterations. b First, mesangial enlargement, where mesangial matrix area was moderately enlarged accompanied with widening of the capillary neck and containing loosely packed extracellular matrices. The number of mesangial cells was unchanged. c Second, mesangial dissolution, where the mesangial matrix area was greatly expanded and characterized by fluid-filled spaces with a small amount of fibrillar components. Glomerular capillaries were almost surrounded by fluid-filled spaces in the mesangial area. d Third, mesangial interposition, where processes of mesangial cells surround individual capillaries circumferentially (*U* urinary space, *P* podocyte, *L* capillary lumen, *MC* mesangial cell; *bars* in the *panels* 10 μm

Table 1 Morphometric analysis of glomeruli. Means±SD (*GBM* glomerular basement membrane)

| | Wild-type 8 w | Null mutant mice 8 w | Wild-type 27 w | Null mutant mice 27 w |
|---|---|---|---|---|
| Glomerular tuft volume ($\times 10^3$ μm$^3$) | 201.9±52.2 | 678.8±123.3[a] | 355.0±59.5[a] | 892.5±257.5[a, b, c] |
| Inner GBM volume | 108.2±10.6 | 418.2±38.2[a] | 200.2±13.4[a] | 633.9±45.9[a, b, c] |
| Capillary volume | 71.0±4.7 | 134.3±15.8[a] | 112.9±15.5[a] | 142.9±28.7[a] |
| Mesangial volume | 37.1±7.9 | 284.0±25.6[a] | 87.3±16.8 | 491.1±71.8[a, b, c] |
| Total GBM surface area ($\times 10^3$ μm$^2$) | 40.8±3.5 | 114.3±14.7[a] | 59.1±8.9 | 97.7±12.9[a, b] |
| Pericapillary GBM surface area | 29.7±1.4 | 66.7±7.1[a] | 40.5±8.6 | 48.5±10.3[a, c] |
| Perimesangial GBM surface area | 11.1±2.6 | 47.6±11.9[a] | 18.6±3.9 | 49.2±4.8[a, b] |

[a] Difference from 8-week wild-type mouse, $P<0.01$
[b] Difference from 27-week wild-type mouse, $P<0.01$
[c] Difference from 8-week AT1a-deficient mice, $P<0.01$


Fig. 7. a, b Dissolution of mesangial area in a null mutant mouse 27 weeks after birth. a Mesangial area was expanded by fluid-filled spaces together with a little extracellular mesangial matrix. Capillary necks were greatly enlarged. *Bar* 10 μm. b High-magnification view of the mesangial area surrounded by the open rectangle in a. The processes of mesangial cells were separated from the glomerular basement membrane and glomerular endothelial cells by fluid-filled spaces, which contained a few fibrillar components. The endothelial cells facing the fluid-filled space were separated from the fluid-filled spaces by an incomplete sheet of basal lamina consisting of electron-dense materials (*arrowheads*). *Bar* 2 μm (*U* urinary space, *L* capillary lumen, *E* glomerular endothelial cell, *MC* mesangial cell, *P* podocyte, *FP* foot process, *GBM* glomerular basement membrane)